



Journal of Wood Science

Mokuzai Gakkaishi (Japanese with English summary) publishes 6 volumes of high-quality scientific information every year.

The journal features original article, note, rapid communication and invited review.

ISSN 1435-0211 / published in Feb, Apr, June, Aug, Oct, Nov /

Journal of Wood Science is edited and published by the Japan Wood Research Society and published by Springer-Verlag Tokyo.

Table of Contents (including previews)

The Latest Issue: Vol.51, No.6

Last update : December 27, 2005 17:31:00

Vol. 52 (2006) No. 1, 2, 3, 4, 5, and 6

Vol. 51 (2005) No. 1, 2, 3, 4, 5, and 6

Vol. 50 (2004) No. 1, 2, 3, 4, 5, and 6

Vol. 49 (2003) No. 1, 2, 3, 4, 5, and 6

Vol. 48 (2002) No. 1, 2, 3, 4, 5, and 6

Vol. 47 (2001) No. 1, 2, 3, 4, 5, and 6

Vol. 46 (2000) No. 1, 2, 3, 4, 5, and 6

Vol. 45 (1999) No. 1, 2, 3, 4, 5, and 6

Vol. 44 (1998) No. 1, 2, 3, 4, 5, and 6



Springer

- [↩ Top / About JWRS](#)
[↩ Enrollment](#)
[↩ Journal](#)
[↩ Annual Meeting](#)
[↩ International Conference](#)
[↩ IAWPS](#)

Volume 51, Number 4 (2005)**Original articles**

Miyuki Takeuchi, Keiji Takabe, Minoru Fujita

Immunolocalization of an anionic peroxidase in differentiating poplar xylem 317

Yoshihiro Hosoo, Masato Yoshida, Takanori Imai, Takashi Okuyama

The effect of day length on diurnal differences in the innermost surface of the S₂ layer in differentiating tracheids 323

Junji Matsumura, Yoko Yamasaki, Kazuyuki Oda, Yoshitake Fujisawa

Profile of bordered pit aspiration in *Cryptomeria japonica* using confocal laser scanning microscopy: pit aspiration and heartwood color 328

Kentaro Abe, Hiroyuki Yamamoto

Mechanical interaction between cellulose microfibril and matrix substance in wood cell wall, determined by X-ray diffraction 334

Anita Firmanti, Efendi Tri Bachtiar, Surjono Surjokusmo, Kohei Komatsu, Shuichi Kawai

Mechanical stress grading of tropical timbers without regard to species 339

Masahiko Kobayashi, Toshiyuki Asano, Mikio Kajiyama, Bunichiro Tomita

Effect of ozone treatment of wood on its liquefaction 348

Dongxiang Wang, Kyoko S. Katsumata, Gyosuke Meshitsuka

Characterization of lignin fragments in alkaline oxygen-stage waste liquor as soil-conditioning agent 357

Tadashi Oikawa, Toshiya Matsui, Yasunori Matsuda, Teruko Takayama, Hitoshi Niinuma, Yasuyo Nishida, Kazuo Hoshi, Mitsuyoshi Yatagai

Volatile organic compounds from wood and their influences on museum artifact materials I: differences in wood species and analyses of causal substances of deterioration 363

Nattaya Lourith, Takeshi Katayama, Toshisada Suzuki

Stereochemistry and biosynthesis of 8-O-4' neolignans in *Eucommia ulmoides*: diastereoselective formation of guaiacylglycerol-8-O-4'-(sinapyl alcohol) ether 370

Nattaya Lourith, Takeshi Katayama, Kimiko Ishikawa, Toshisada Suzuki

Biosynthesis of a syringyl 8-O-4' neolignan in *Eucommia ulmoides*: formation of syringylglycerol-8-O-4'-(sinapyl alcohol) ether from sinapyl alcohol 379

Morten Eikenes, Gry Alfredsen, Bjorn Erik Christensen, Holger Militz, Halvor Solheim

Comparison of chitosans with different molecular weights as possible wood preservative 387

Eiji Minami, Shiro Saka

Decomposition behavior of woody biomass in water-added supercritical methanol 395

Notes

Jonas Blomberg

Elastic strain at semi-isostatic compression of Scots pine (*Pinus sylvestris*) 401

Oner Unsal, Nadir Ayrilmis

Variations in compression strength and surface roughness of heat-treated Turkish river red gum (*Eucalyptus camaldulensis*) wood 405

Hulya Kalaycioglu, Ilhan Deniz, Salim Hiziroglu

Some of the properties of particleboard made from paulownia 410

Jianying Xu, Ragil Widyorini, Shuichi Kawai

Properties of kenaf core binderless particleboard reinforced with kenaf bast fiber-woven sheets 415

Rapid communications

Shin-ichiro Tohmura, Kohta Miyamoto, Akio Inoue

Acetaldehyde emission from glued-laminated timber using phenol-resorcinol-formaldehyde resin adhesives with addition of ethanol 421

Zhenfu Jin, Yuji Matsumoto, Takeshi Tange, Takuya Akiyama, Masanobu Higuchi, Tadashi Ishii, Kenji Iiyama

Proof of the presence of guaiacyl-syringyl lignin in *Selaginella tamariscina* 424

Announcement 427

ORIGINAL ARTICLE

Anita Firmanti · Efendi Tri Bachtiar
Surjono Surjokusumo · Kohei Komatsu · Shuichi Kawai

Mechanical stress grading of tropical timbers without regard to species

Received: March 12, 2004 / Accepted: June 22, 2004

Abstract Some reports have shown that for single species the correlation between modulus of elasticity (MOE) and modulus of rupture (MOR) in bending is quite high. Tropical timbers consist of hundreds of species that are difficult to identify. This report deals with the mechanical stress grading of tropical timber regardless of species. Nine timber species or groups of species with a total number of 1094 pieces measuring $60 \times 120 \times 3000$ mm, were tested in static bending. The MOE was measured flat wise, while MOR was tested edge wise. Statistical analysis of linear regression with a dummy model and analysis of covariance were used to analyze the role of MOE and the effect of species on prediction of MOR. The analysis showed that using MOE as a single predictor caused under/overestimation for one or more species and/or groups of species. The accuracy of prediction would be increased with species identification. An allowable stress and reference resistance for species and/or groups of species were provided to compare with the prediction of strength through timber grading. The timber strength class for species and/or groups of species was also established to support the application of mechanical timber grading.

Key words Regardless of species · Mechanical stress grading · Tropical timbers · Allowable stress · Reference resistance

Introduction

Being a natural material, wood has large variations of strength and stiffness properties among species and even among pieces in one species. The variations of strength and stiffness are caused by defects or imperfections like knots (number, size, and location in each piece of timber), slope of grain, and interlocked grain. To guarantee structural safety, prediction of timber strength is necessary. The strength characteristics of a piece of timber should be evaluated by nondestructive methods. It can be done through visual grading or mechanical grading or by combination of such methods. For simplicity and economy, pieces of timber of similar mechanical properties are placed in categories called stress grades.

Most tropical countries are blessed with a biodiversity of natural resources which means that hundreds or thousands of timber species are available for construction. In such cases, the application of visual grading is complicated due to the difficulties of species identification and checking of the imperfection condition. Predicting the strength of wood on a large scale through density shows a poor coefficient of determination (R^2). A study on Norway spruce (*Picea abies*) reported that the R^2 value of the relationship between density and bending strength was in the range of 0.16–0.40 while the R^2 value of the relationship between the density and knots was 0.38. However, the stiffness, which is normally expressed as the modulus of elasticity (MOE), is by far recognized as the best predictor of strength.¹ The most common method of sorting machine-graded lumber is to measure MOE.¹ The R^2 value of the relationship between MOE and bending strength [modulus of rupture (MOR)] of Norway spruce was in the range of 0.51–0.72.^{2,3} Previous studies have showed the R^2 value between MOE in flatwise timber and MOR was 0.61 for *Acacia mangium* timber and 0.53 for mixed tropical wood.² Combining MOE with knots and other data gained slight improvement in the relationship between MOE and MOR.²

In the application to timber grading and strength classes, the strength of a piece of timber regardless of species could be predicted and classified through measuring the

A. Firmanti
Research Institute For Human Settlements, Jl. Panyauangan-Cileunyi
Wetan, Bandung 40008, Indonesia

E.T. Bachtiar · S. Surjokusumo
Faculty of Forestry, Bogor Agriculture University, Kompleks IPB
Darmaga Bogor 16680, Indonesia

K. Komatsu · S. Kawai (✉)
Research Institute for Sustainable Humanosphere, Kyoto University,
Uji 611-0011, Japan
Tel. +81-774-38-3673; Fax +81-774-38-3678
e-mail: skawai@rish.kyoto-u.ac.jp

MOE. Most species are grouped together and the timber performances from such species are treated similarly. With reference to the availability of timber for structural purposes consisting of many species in tropical countries, the application of mechanical stress grading needs to be evaluated.

The objective of this study was to evaluate the application of mechanical grading to tropical timber, which consists of timber from natural forest, timber from plantation forest, hardwood as well as softwood. It is expected that the results can be utilized in structural timber design.

Materials and methods

The number of the specimens was 1094 pieces of tropical wood consisting of timber from natural forest [60 pieces of kapur (*Dryobalanops aromatica* Gaertner f.), 192 pieces of a group of meranti or *Shorea* sp., and 314 pieces of mixed unknown species namely "borneo" timber] hardwood from plantation forest [120 pieces of *Acacia mangium*, Willd., 60 pieces of *falcata* (*Paraserianthes falcataria*, L. Nielsen), 60 pieces of rubber wood (*Hevea brasiliensis*, Willd), and 60 pieces of *Maesopsis eminii*, Engler], and softwood from plantation forest [168 pieces of *Pinus merkusii*, Junghuhn & de Vriese, and 60 pieces of agathis (*Agathis damuhara*, Lambert Rich)]. The specimens were 60 × 120 × 3000 (L) mm when air-dried. For any piece of lumber, the imperfection condition was evaluated based on the visual grading system of Indonesian Standard for Construction Timber (SNI 03-3527).⁶ Based on the diameter of the knots, slope of the grain, length of the wane, and other visual grading parameters, the timber was classified into the three categories of class A, class B, and that rejected as structural timber. Only timber that was classified as timber suitable for building construction was used as specimens.

The MOE in flatwise configuration with center-point loading was measured using a simple machine with a deflectometer that can magnify the reading about 40 times. In the measurement of MOE flat wise, the span was 2730 mm and the applied load was 25 kg. Before measuring the MOE flat wise, the machine was calibrated based on a certified dial gauge. The specimens were then tested in flexural bending with three-point loading edge wise with a universal testing machine with a capacity of 100 tons, following the procedure of ASTM D 198.⁷ With consideration of the loading system, adjustment factors were applied to the MOE and MOR calculations based on the equilibrium moisture content in Indonesia of 15% and ASTM 2915.⁸

Regression analysis was used to analyze the relationship between MOE flat wise and MOR of the timber. Based on the regression analysis, the allowable stress for the tropical wood and the stress classification were established. The effects of timber species on the MOR of timber were analyzed using analysis of covariance (ANCOVA) with MOE as the covariant variable and the model as shown in Eq. 1:

$$Y_{ij} = \mu + \tau_i + \beta(X_{ij} - \bar{X}) + \varepsilon \quad (1)$$

where Y_{ij} is the measured MOR of species i and sample number j , μ is the average MOR, τ_i is the additive effect of species, β is the regression coefficient that expresses the dependency of MOR on MOE, X_{ij} is the measured MOE, \bar{X} is the average MOE, and ε_{ij} is the error of sample number j of species i .

The hypothetical test was conducted through an F test by considering:

$H_0: \tau_i = 0$, there is no significant effect of species or group of species to MOR.

For

$H_1: \tau_i \neq 0$, there is at least one species that shows a significantly different MOR value to the others.

The prediction of strength characteristics of the timber was analyzed through a model as described by Eq. 2:

$$Y_{ij} = z_{ij}a_j + f(X_{ij}) + \varepsilon_{ij} \quad (2)$$

where z_{ij} is the dummy variable of species i , a_j is a constant of the dummy variable and, $f(X_{ij})$ is a function of the relationship between MOR and MOE. Two hypotheses were used as:

1. $H_0: \beta_1 = \beta_2 = \beta_3 \dots = \beta_k = 0$, species and MOE provide no significant effect to MOR.
 $H_1: \exists \beta_k \neq 0$, at least one species and/or MOE provide significant effect to MOR.
2. H_0 : species provide no significant effect on MOR when MOE is included in the analytical model.
 H_1 : at least one species provides significant effect on MOR when MOE is included in the analytical model.

Strength characteristics based on the allowable stress design (ASD) and load and resistance factor design (LRFD) were established following ASTM D 2915⁸ and ASTM D 5457,⁹ respectively.

Results and discussion

Modulus of elasticity and bending strength performance of the timber

MOE and MOR of timber are the two parameters usually used in the evaluation of the bending performance of timber in structural sizes. The MOE and MOR of timber may vary among the species, trees, logs, and even among the sawn timber of one log.¹⁰ Variations of strength and stiffness are, in general, caused by density and imperfections, i.e., knots, slope of grain, and interlocked grain.

The lowest value of MOE was 4.1 GPa found in *Acacia mangium* from the plantation forest and the highest was 28.5 GPa found in mixed unknown timber from natural forest as shown in Table 1. The weakest value of MOR was 10.8 MPa found in agathis from plantation forest and the strongest was 134.3 MPa found in shorea sp. from natural forest. Generally, the range of MOE and MOR values of timber from natural forest is wider than that of timber from

Table 1. Modulus of elasticity (MOE) and modulus of rupture (MOR) performance of tested timber

Specimens	MOE (Gpa)				MOR (MPa)				Moisture content (%)			
	Min.	Max.	Mean	SD	Min.	Max.	Mean	SD	Min.	Max.	Mean	SD
Hardwood from natural forest	5.3	28.5	15.1	4.1	13.8	134.3	59.8	20.3	13.9	18.4	15.5	1.4
Borneo timber	8.3	28.5	15.3	4.1	30.0	108.0	62.8	15.4	14.3	18.4	15.5	1.5
Shorea sp.	5.3	25.9	14.9	3.9	13.8	134.3	55.1	26.1	13.9	16.7	14.9	1.3
Kapur	8.4	28.3	14.2	4.7	23.0	107.6	56.1	22.2	14.1	17.9	16.1	1.3
Planted fast-growing hardwood	4.1	22.1	9.8	2.9	11.6	92.0	41.6	13.1	12.9	18.8	15.6	1.1
<i>Acacia mangium</i>	4.1	15.8	8.9	2.6	11.6	92.0	42.2	15.8	12.9	16.8	15.2	1.2
Falcata	6.2	13.0	8.7	1.4	15.3	48.0	32.7	8.1	13.2	17.9	14.8	0.9
Rubber wood	6.3	17.6	10.6	3.0	29.4	56.7	43.9	7.9	14.4	18.7	16.3	1.0
<i>Maesopsis eminii</i>	5.5	22.1	12.0	3.4	28.5	70.8	45.8	10.2	13.9	18.8	16.2	1.4
Total hardwood	4.1	28.5	13.6	4.5	11.6	134.3	54.7	20.1	12.9	18.8	15.6	1.2
Planted fast-growing softwood	5.6	21.7	12.6	3.3	10.8	67.2	37.1	11.8	13.8	18.7	15.8	1.2
<i>Pinus merkusii</i>	5.6	21.7	12.9	3.6	15.4	55.9	34.2	8.6	14.5	17.6	15.9	1.0
Agathis	7.6	16.6	12.0	2.3	10.8	67.2	44.6	12.3	13.8	18.7	15.7	1.3
Tropical timber (total)	4.1	28.5	13.3	4.3	10.8	134.3	50.6	20.0	12.9	18.8	15.7	1.1

SD, standard deviation

Table 2. Goodness of fit (percent) of parametric distribution to the plots of tropical timber

Specimens	MOE			MOR		
	Normal	Log-normal	Weibull	Normal	Log-normal	Weibull
Timber from natural forest	67	100	47	84	68	100
Borneo timber	69	100	56	100	51	56
Shorea sp.	100	79	92	55	100	73
Kapur	60	100	50	71	100	72
Planted fast-growing hardwood	85	85	100	97	100	98
<i>Acacia mangium</i>	100	100	71	65	100	69
Falcata	85	80	100	100	86	100
Rubber wood	65	100	56	95	100	86
<i>Maesopsis eminii</i>	69	100	55	88	100	82
Hardwood	84	99	100	90	100	100
Planted fast-growing softwood	100	87	75	66	100	60
<i>Pinus merkusii</i>	100	91	87	91	100	73
Agathis	94	83	100	100	82	90
Tropical timber (total)	91	96	86	73	100	86

plantation forest. The wide range of such values of timber from natural forest may be due to the cultivation system. Shorea sp. is a group of species occurring in the mixed unknown tropical wood commonly known as "Borneo" timber. It is reasonable to expect that the range of MOE and MOR of mixed tropical timber is wider than that of timber from plantation forest where the trees are well cultivated and homogenous.

Parametric distributions, namely, normal, log-normal, and Weibull distributions were applied to evaluate the distribution. Based on the frequency analysis, the apparent distribution was also analyzed to obtain the goodness of fit of the parametric distributions, i.e., normal distribution, log-normal distribution, and the cumulative Weibull distribution.¹¹ It is not easy to recognize the fit of the parametric distributions to the actual frequency plots of the timber

generalized for all timber. Some species have a high goodness of fit to the normal distribution, some to the log-normal distribution, and others to the Weibull distribution as shown in Table 2. The parametric distribution and actual frequency of the MOE and MOR of the tropical timber are shown in Figs. 1 and 2. Selecting the best fit distribution for the actual frequency values is important, especially for the lower tail values in the establishment of allowable MOE and MOR. In ASTM D 5457, the distribution of timber is assumed to be a Weibull distribution while the European standard tends to assume a log-normal distribution.¹² With reference to Fig. 1, for the lower tail values, the log-normal and Weibull distributions provide better fits than the normal distribution, but for the other plots the log-normal distribution seems better than the Weibull distribution.

Table 3. The parameters of parametric distribution and their fifth percentile limit

Specimens	MOE						MOR					
	Log-normal			Weibull			Log-normal			Weibull		
	λ	ξ	$R_{0.05}$	η	α	$R_{0.05}$	λ	ξ	$R_{0.05}$	η	α	$R_{0.05}$
Timber from natural forest	2.68	0.26	9.1	16.5	4.5	9.3	4.04	0.33	29.8	66.6	3.4	26.5
Borneo timber	2.69	0.26	9.4	16.8	4.6	9.6	4.11	0.24	39.4	68.5	4.9	38.7
Shorea sp.	2.67	0.26	8.8	16.3	4.4	8.5	3.91	0.45	20.7	62.2	2.5	20.6
Kapur sp.	2.60	0.32	7.8	15.7	3.8	8.5	3.95	0.38	26.6	62.7	3.0	28.8
Planted fast-growing hardwood	2.24	0.30	5.7	10.8	4.1	5.3	3.68	0.31	22.4	46.2	3.6	21.3
<i>Acacia mangium</i>	2.15	0.28	5.1	9.8	4.2	4.9	3.68	0.36	19.6	47.2	3.1	16.3
Falcata	2.16	0.16	6.5	9.4	6.8	6.6	3.46	0.24	19.5	36.0	4.2	17.9
Rubber wood	2.32	0.27	6.2	11.6	4.3	6.0	3.77	0.18	30.9	47.1	6.4	31.2
<i>Maesopsis eminii</i>	2.45	0.37	7.2	13.2	4.4	7.7	3.80	0.22	30.0	49.5	5.3	30.5
Hardwood	2.56	0.33	7.2	15.1	3.6	7.0	3.94	0.36	26.3	61.1	3.2	24.2
Planted fast-growing softwood	2.51	0.25	7.8	13.8	4.7	7.6	3.56	0.31	19.8	41.1	3.7	19.6
<i>Pinus merkusii</i>	2.52	0.27	7.6	14.2	4.3	7.3	3.50	0.25	21.2	37.4	4.7	21.3
Agathis	2.47	0.19	8.4	12.9	6.2	8.4	3.74	0.33	18.7	50.1	2.7	14.2
Tropical timber (total)	2.54	0.32	7.2	14.7	3.8	7.1	3.85	0.38	23.5	56.6	3.1	22.8

λ , Mean of log-normal distribution; ξ , standard deviation of log-normal distribution; η , scale parameter of Weibull distribution; α , shape parameter of Weibull distribution; $R_{0.05}$, fifth percentile limit

Fig. 1a-c. Parametric distributions of modulus of elasticity (MOE) for group of species of tropical timbers. **a** Normal distribution, **b** log-normal distribution, **c** Weibull distribution

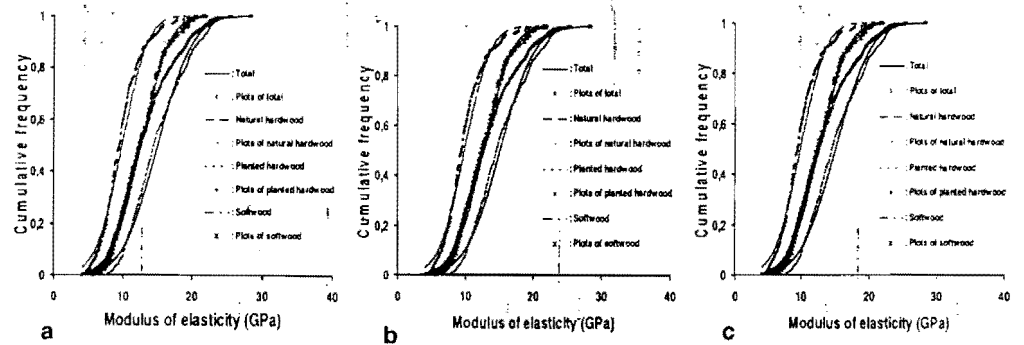
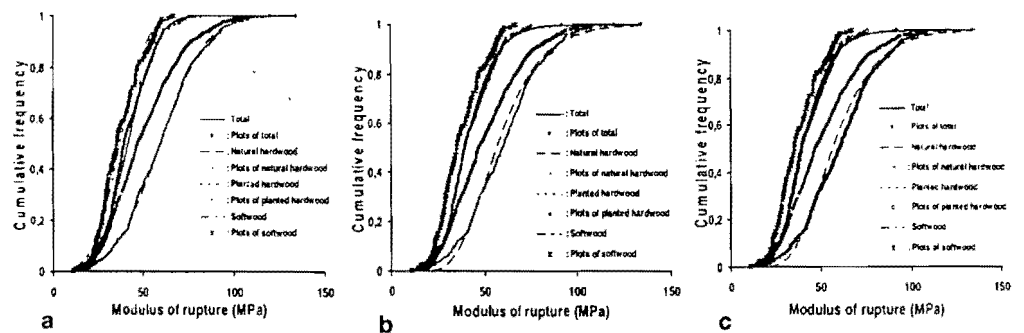


Fig. 2a-c. Parametric distributions of modulus of rupture (MOR) for group of species of tropical timbers. **a** Normal distribution, **b** log-normal distribution, **c** Weibull distribution



For each species or group of species, the mean and the standard deviation of the log-normal distribution, the shape and scale parameter of the Weibull distribution, as well as the fifth percentile limit were calculated and are presented in Table 3. An observation to the lower tail of the distribution is important in order to reduce error in the establishment of allowable stress. Although the goodness of fit of the parametric distributions to the actual frequency of MOE

and MOR of the timber could not be specified as shown in Table 2 and Figs. 1 and 2; the difference of the fifth percentile limit of both the log-normal and Weibull distributions were relatively small as shown in Table 3. As described above, the fifth percentile limit of the MOE and MOR of timber from natural forest was also higher than planted timber. The MOE of planted softwood was higher than that of planted hardwood, while the strength of planted hard-

Table 4. The allowable bending stress (in MPa) for allowable stress design (ASD)

Specimens	Parametric (distribution)		Nonparametric		
	5% PE Weibull	5% PE log-normal	5% PE	5% TL	δ
Timber from natural forest	12.62	14.19	13.09	12.62	0.036
Borneo timber	18.43	18.76	19.48	18.10	0.071
Shorea sp.	9.81	9.86	9.90	9.48	0.042
Kapur	13.71	12.67	14.75	14.52	0.015
Planted hardwood	10.14	10.67	10.71	10.38	0.032
<i>Acacia mangium</i>	7.76	9.33	8.57	7.86	0.083
Falcata	8.52	9.29	8.43	8.19	0.030
Rubber wood	14.86	14.71	15.26	15.10	0.010
<i>Maesopsis eminii</i>	14.52	14.29	14.86	14.43	0.028
Hardwood	11.52	12.52	11.62	11.48	0.011
Softwood	9.33	9.43	9.29	8.95	0.028
<i>Pinus merkusii</i>	10.14	10.10	10.38	10.14	0.022
Agathis	6.76	8.90	7.04	6.62	0.061
Topical timber (total)	10.86	11.19	10.91	10.76	0.014

PE, point estimate; TL, tolerance limit; δ , relative difference between nonparametric point estimate (NPE) and nonparametric lower tolerance limit (NTL) which was expressed as $(NPE-NTL)/NPE$

wood was higher than that of planted softwood. These properties may be affected by the different characteristics of the timbers. Two distinct conditions that might affect MOE and MOR are the presence of tracheid in softwoods and vessels in hardwoods and the different formations of knots in both.¹²

Establishment of allowable stress and reference resistance in LRFD of species or group of species

The basic concept of ASD is that the working stress in the member of a structure should be lower or the same as the product of allowable stress of the member and corresponding duration of loading.⁹ The allowable stress is the strength characteristic with the reduction of the safety factor. For example, in Indonesia, as well as in the USA, the safety factor of bending strength is 1/2.1.^{8,13} Based on ASTM⁸ and European Standards,¹⁴ the strength characteristic of the timber is the fifth exclusion limit ($R_{0.05}$) of the population distribution. The strength characteristic of timber is analyzed using parametric and/or nonparametric procedures.⁸

As mentioned above, the distributions of the timber could not be easily distinguished. For parametric procedures, the allowable strength of timber species and group of species could be obtained from Table 3 with reference to Table 2 for the goodness of fit. There are two statistical ways for nonparametric procedures, i.e., nonparametric point estimate (NPE) based on interpolated data, and nonparametric lower tolerance limit (NTL) based on order statistics. The width of the confidence interval is a sufficiently small fraction of the mean with the values in the range of 0.016 to 0.067. In such a condition, the allowable value of modulus of elasticity is the mean of MOE as shown in Table 1.⁷

Through parametric and nonparametric procedures with the condition as mentioned above and considering the safety factor of bending in 10 years loading of 2.1,^{8,13} the

strength characteristic and allowable strength is presented in Table 4. With the sufficiently small values of the relative difference between NPE and NTL, the value of NPE as shown in Table 4 is the allowable stress for bending.⁸ The allowable stress of any species or group species could also be established through parametric procedures with the small difference value between parametric point estimate (PPE) and NPE or NTL.

The reference resistance for LRFD of the timber was calculated based on the format conversion and reliability normalization factor as mentioned in ASTM D 5457.⁹ Format conversion used the ASD load duration adjustment factor of 1.15, LRFD time effect factor of 0.80, and specified LRFD factor for bending of 0.85.⁸ The calculation based on reliability normalization factor was conducted using an assumption that the distribution was a Weibull distribution, although the goodness of fit of the Weibull distribution for some species or group of species were lower than 100% as shown in Table 2. In the reliability normalization factor procedure, sample size and coefficient of variations are the decisive factors.

The reference resistance of a species or group of species established through format conversion seemed higher than the one through reliability normalization as shown in Table 5. When the coefficient of variation of the strength of a species is relatively high, the reference resistance based on the reliability normalization would be much lower than the one from format conversion due the reverse position of the coefficient of variation in the reliability normalization equation. Such phenomena indicate that the application of LRFD based on the reliability normalization factor for tropical timbers needs more study.

With reference to Tables 1, 4, and 5, the application of allowable stress and reference resistance for species and/or group of species will mean very safe but inefficient use of the timber due to the use of the fifth percentile of the distributions and/or statistical nonparametric values as the predicted values.

Table 5. Reference resistance of the bending strength (MPa) of timber for load and resistance factor design (LRFD) based on ASTM D 5457

Specimens	Format conversion				Reliability normalization
	Parametric		Nonparametric		
	5% PE Weibull	5% PE log-normal	5% PE	5% TL	
Timber from natural forest	32.05	36.04	33.25	32.05	26.71
Borneo timber	46.81	47.65	49.48	45.97	41.95
Shorea sp.	24.92	25.04	25.15	24.08	16.83
Kapur	34.82	32.18	37.47	36.88	20.70
Planted hardwood	25.76	27.10	27.20	26.37	18.98
<i>Acacia mangium</i>	19.71	23.70	21.77	19.96	16.60
Falcata	21.64	23.60	21.41	20.80	17.19
Rubber wood	37.74	37.36	38.76	38.35	33.51
<i>Maesopsis eminii</i>	36.88	36.30	37.74	36.65	29.99
Hardwood	29.26	31.80	29.51	29.16	23.41
Softwood	23.70	23.95	23.60	22.73	17.36
<i>Pinus merkusii</i>	25.76	25.65	26.37	25.76	22.18
Agathis	17.17	22.61	17.80	16.81	14.27
Tropical timber (total)	27.58	28.42	27.71	27.33	20.93

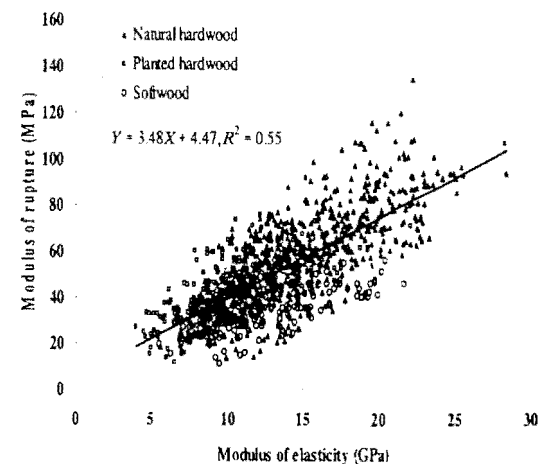
Table 6. The coefficient of determination of the relationship between MOE and MOR

Specimens	Number of samples	Coefficient of determination (R^2)
Timber from natural forest	566 ²	0.56
Borneo timber	314 ²	0.53
Shorea sp.	192	0.64
Kapur	60	0.71
Planted hardwood	300	0.57
<i>Acacia mangium</i>	120	0.71
Falcata	60	0.63
Rubber wood	60	0.61
<i>Maesopsis eminii</i>	60	0.64
Planted softwood	228	0.36
<i>Pinus merkusii</i>	168	0.60
Agathis	60	0.68

Application grading regardless of species conception for the tropical timber

Some difficulties appeared when visual grading the tropical timber due to the variety of timber species and their embedded characteristics. Shorea sp. consists of 194 species of which 163 species are found in Melanesia.¹⁵ It was also reported that from 400 pieces of mixed tropical timber, namely "Borneo," 25 species were found with a wide range of density and strength of the timber.⁵ Visual grading for predicting the strength through evaluation of imperfections, being expressed as the "strength ratio" of clear straight-grain, small specimens of a species, is difficult to apply to the tropical species in such conditions.

The MOE is by far the best predictor of MOR.² Some studies of single species reported a relatively strong relationship between MOE and MOR of the timber.²⁻⁵ Table 6 shows the relationship between MOE flat wise and strength of the timber of some species and groups of species. The coefficient of determination (R^2) of the relationship between MOE and MOR of the known single species was in the range of 0.60 to 0.71, but it was lower for the mixed species. When all of the specimens were taken into account,

**Fig. 3.** Relationship of MOE and MOR for group of species of tropical timbers

the R^2 value was 0.55 as shown in Fig. 3. The R^2 value of softwood represented by *Pinus merkusii* and agathis was 0.36. Although the value was quite small, it was better than combining the data of *Pinus merkusii* with falcata of which

Table 7. Equations for predicted MOR based on MOE of the timber species

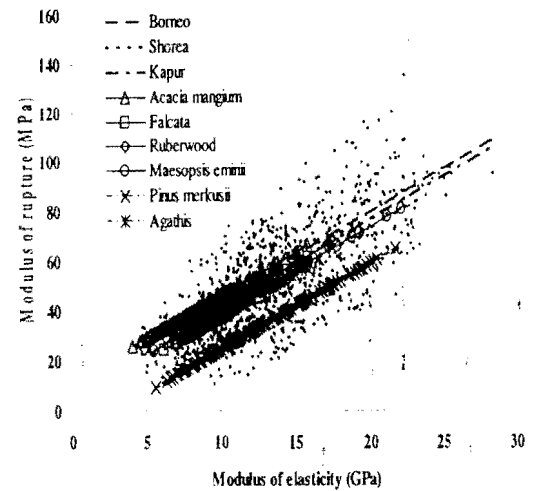
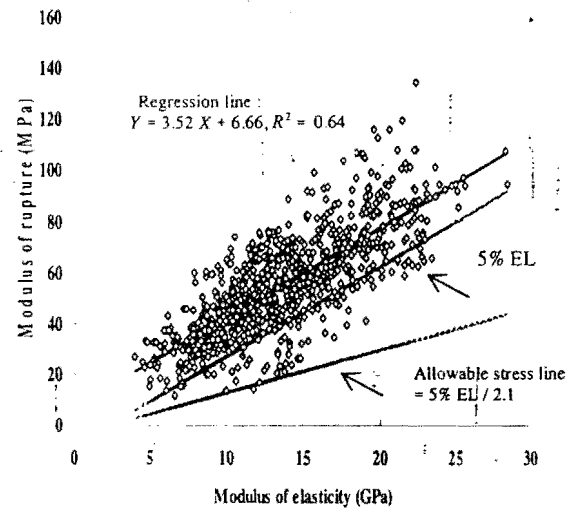
Specimens or group of specimens	Regression line
Borneo	MOR = 10.67 + 3.11 MOE
Shorea sp.	MOR = 4.41 + 3.11 MOE
Kapur	MOR = 7.64 + 3.11 MOE
<i>Acacia mangium</i>	MOR = 11.86 + 3.11 MOE
Falcata	MOR = 2.86 + 3.11 MOE
Rubber wood	MOR = 7.54 + 3.11 MOE
<i>Maesopsis eminii</i>	MOR = 4.76 + 3.11 MOE
<i>Pinus merkusii</i>	MOR = 9.69 + 3.11 MOE
Agathis	MOR = 3.87 + 3.11 MOE

the mean value of the strength was similar to those of *Acacia mangium*, rubber wood, and *Maesopsis eminii* from the hardwood. The R^2 value of the relationship between MOE and MOR of such a combination was less than 0.30.

Because the R^2 value of MOE and MOR of all timber specimens in this experiment was 0.55, MOE is a good predictor of MOR, although the application of using MOE as a single variable would cause the over/underestimation of MOR, at least for one species as expressed by the high value of allowable stress F calculated and a very small significant value. The hypothesis that at least there is a species providing a MOR value significantly different from others could be accepted. The fact that there is at least one species providing significantly different MOR endorsed that the identification of the timber species will improve the prediction of MOR through MOE from 74.2% ($R^2 = 0.55$) to the range of 77.5% ($R^2 = 0.60$) to 84.3% ($R^2 = 0.71$).

The prediction equation of MOR based on MOE was obtained through the regression dummy analysis with matrix variables for species and/or group of species. It was found that species and group of species and/or MOE gave a significant effect on MOR with the high calculated value of F and very small significant value. The hypothesis that at least one species and/or MOE provide significant effect on the MOR is accepted. The regression line of the species and group of species is shown in Table 7 and Fig. 4. Using MOE as the strength predictor regardless of species will overestimate MOR for softwood, especially *Pinus merkusii*, as shown in Fig. 4.

Although the timber from natural forest is still dominant in the timber construction industries in some tropical areas, promotion of the utilization of planted timber, especially fast growing species, has been disseminated for some decades. Because the selection cutting policy has been applied since the early 1980s, the availability of some selected species for timber construction has decreased. In many cases, rough visual grading and small clear specimen test results have been applied for predicting the strength of the timber. For the unknown species from natural forest, it is classified as a second class timber although it covers a wide range of strength. The utilization of timber from fast growing trees is not yet popular due to the opinions on such timber as being of low grade for construction. With such background, the application of mechanical timber stress

**Fig. 4.** Regression line of MOE and MOR for species and group of species of tropical timbers**Fig. 5.** Regression line, 5% exclusion limit, and allowable stress line of tropical hardwood

grading to tropical planted timber, based on MOE with regard to and/or regardless of species is very important.

Establishment of timber strength classes

Although the regression line of agathis is close to hardwood as shown in Fig. 4 and Table 7, there is a tendency for MOE to predict lower values of MOR than those of hardwood. With consideration that *Pinus merkusii* and agathis would be overestimated, the timber strength classes regardless of species was established only for hardwood with the regression line and the 5% exclusion limit as shown in Fig. 5. Exclusion of the values of softwood from the equation as shown in Fig. 3 improved the relationship of MOE and MOR to 0.64 as shown in Fig. 5. The strength classes of timber were derived based on 5% Exclusion limit ($R_{0.05}$) of ASD and LRFD as shown in Table 8. The reference resistance was estimated through format conversion with a load

Table 8. Timber strength classes for ASD and LRFD based on mechanical stress grading for tropical hardwood timber regardless of species

Grade	MOE (GPa)	Allowable stress (MPa)	Reference resistance (MPa)
E 255	25.5	37.3	94.8
E 240	24.0	34.1	86.7
E 225	22.5	32.2	81.8
E 210	21.0	30.0	76.2
E 195	19.5	27.4	69.6
E 180	18.0	25.2	64.1
E 165	16.5	22.8	57.9
E 150	15.0	20.3	51.7
E 135	13.5	17.9	45.5
E 120	12.0	15.5	39.3
E 105	10.5	13.0	33.1
E 90	9.0	10.6	26.9
E 75	7.5	8.2	20.7
E 60	6.0	5.7	14.5

adjustment factor of 1.15, a LRFD time factor of 0.80, and a ratio of live to dead load effects of 3, and specified a LRFD resistance factor for bending of 0.85. The format conversion reference resistance is computed with the design equation⁹ as below:

$$\text{LRFD: } \lambda \phi R_n \geq 1.2D + 1.6L$$

$$\text{ASD: } K_d F_n \geq D + L$$

where λ is the time effect factor, ϕ is the resistance factor, R_n is the reference resistance, D and L are the dead and live load effects, respectively, K_d is the load duration factor (for ASD), and F_n is the allowable stress (for ASD).

The format conversion reference resistance is computed by multiplying the ASD resistance by the format conversion factor (K_1), where it is calculated as:

$$K_1 = (R_n / F_n) \phi$$

where ϕ is the specified LRFD resistance factor.

The proposed strength classes of the timber provides wider strength classes than common grades for machine-graded lumber established by the American Forest Product Society⁷ and the Japanese standard for timber structures.¹⁶ The upper parts of the proposed strength classes are occupied by the hardwood from natural forest which is usually cut at over 35 years while the planted hardwood is mostly cut at between 10 and 25 years, depending on the species and the purpose of the plantation. With reference to Tables 4 and 5, the allowable stiffness and strength properties of planted hardwood timber are almost the same as those of softwood in subtropical areas.¹⁶

In practical application, timber identification is not easy, especially for mixed tropical wood and shorea sp., which consists of hundreds species. Therefore, timber strength classes that are regardless of species are desirable. When a timber species is not well recognized by designers, the timber strength classes that are regardless of species as shown in Table 8 should be applied because they are more conservative than the strength classes for specific species as shown in Table 9. With various species in a group, the

timber strength classes for a group of species, namely "Borneo" and shorea sp., were not provided. In the design stage, the timber strength classes that are regardless of species as mentioned above and shown in Table 8 should be applied for such groups.

Conclusion

Timber is a natural material with the embedded properties from the tree and those obtained during the production process. The MOE and MOR of timber were in wide ranges and the distributions of the mechanical performances did not clearly fit one parametric distribution, i.e., normal, log-normal, or Weibull distribution. The allowable stress for timber produced inefficient prediction. To effectively utilize timber as a structural material, timber grading can be applied visually and/or mechanically. With various timber species available and technical difficulties in applying visual grading, mechanical grading with MOE as the predictor has been studied with regard to and regardless of species.

The ANCOVA statistical analysis showed that using MOE as a single variable for predicting MOR caused under/overestimation for one or more species and/or groups of species. The percentage of the accuracy of prediction would be increased with species identification. The analysis model with dummy regression found that at least one or more species showed a significant effect on MOR. It was also found that *Pinus merkusii*, as a tropical softwood, produced a significantly different MOR for the same MOE when compared with other timber.

The hardwood timber strength classes had been proposed to support the application of mechanical timber stress grading. To anticipate the application of the LRFD concept in global development, a reference resistance based on stress-graded timber has also been established through more research studies in strength characteristics of tropical timber.

Table 9. Timber strength classes for ASD and LFRD based on mechanical stress grading of some tropical timber species

Species name	Grade	MOE (Gpa)	Allowable stress (Mpa)	Reference resistance (Mpa)
Kapur	E 225	22.5	32.2	81.7
	E 210	21.0	29.7	75.5
	E 195	19.5	27.3	69.4
	E 180	18.0	24.9	63.2
	E 165	16.5	22.4	57.0
	E 150	15.0	20.0	50.8
	E 135	13.5	17.5	44.6
	E 120	12.0	15.2	38.4
<i>Acacia mangium</i>	E 150	15.0	25.2	63.9
	E 135	13.5	22.7	57.7
	E 120	12.0	20.3	51.5
	E 115	10.5	17.8	45.4
	E 90	9.0	15.4	39.2
	E 75	7.5	13.0	33.0
	E 60	6.0	10.5	26.8
Falcata	E 150	15.0	22.2	56.3
	E 135	13.5	19.7	50.2
	E 120	12.0	17.3	43.9
	E 105	10.5	14.9	37.8
	E 90	9.0	12.4	31.6
Rubber wood	E 165	16.5	26.6	67.7
	E 150	15.0	24.2	61.5
	E 135	13.5	21.8	55.3
	E 120	12.0	19.3	49.1
	E 105	10.5	16.9	43.0
	E 90	9.0	14.5	36.8
<i>Maesopsis eminii</i>	E 210	21.0	31.8	80.7
	E 195	19.5	29.3	74.5
	E 180	18.0	26.9	68.3
	E 165	16.5	24.5	62.2
	E 150	15.0	22.0	56.0
	E 135	13.5	19.6	49.8
	E 120	12.0	17.2	43.6
	E 105	10.5	14.7	37.4

Acknowledgments The authors sincerely acknowledge the financial support of the Research Institute for Human Settlement of Indonesia. The invaluable support of A/Prof. M. Sato of Global Agricultural Sciences, Graduate School of Agricultural and Life Sciences, The University of Tokyo, Japan, is highly appreciated.

References

- Kretschmann DE, Green DW (1999) Lumber stress grades and allowable properties. Wood handbook: wood as an engineering material. Forest Product Laboratory U.S. Department of Agriculture, Washington, DC, Chapter 6, pp 6.1–6.14
- Johanson CJ (2002) Grading of timber with respect to mechanical properties. Timber engineering. Wiley, New York, pp 23–43
- Steffen A, Johansson CJ, Wormuth EW (1997) Study in the relationship between flat-wise and edge-wise moduli of elasticity of sawn timber as a means to improve mechanical strength grading technology. Holz Roh Werkst 55:245–253
- Firmanti A, Surjokusumo S, Komatsu K, Kawai S (2004) The establishment of strength characteristic of fast growing acacia mangium timber for structural materials. (Submitted)
- Firmanti A (1996) Basic concept of timber grading in Indonesia. Journal Masalah Bangunan, 36:1–4, 7–11
- Indonesian Standardization Board (1994) Standard quality of timber for building structure (in Indonesian). SNI 03-3527-2, Jakarta
- ASTM Standard D 198-1999 (2000) Standard test methods of static tests of lumber in structural sizes Vol 04.10, Wood, Philadelphia
- ASTM Standard D 2915-1997 (2000) Evaluating allowable properties for grades of structural timber, Vol 04.10, Wood, Philadelphia
- ASTM Standard D-5457 (1997) Standard specification for computing reference resistance of wood based materials and structural connections for load and resistance factor design, Vol 04.10, Wood, Philadelphia
- Gloss P (1993) Strength grading. Step Eurofortech Lecture, 6 A6:1–8
- Horie K (1997) The statistical and probability method of timber strength data (in Japanese). Timber Engineering Institute, Sunagawa-Hokkaido, Japan
- Brown HP, Panshin AJ, Forsaith CC (1949) Text book of wood technology. Structure, identification, defects, and uses of the commercial woods of the United States, vol 1 McGraw-Hill, New York, pp 111–285
- Indonesian Standard Board (2002) Code of practice for timber construction (in Indonesian). SNI 03-3971, Jakarta
- European Committee for Standardization (1995) EN 384: Structural timber – determination of characteristic value of mechanical properties and density, Brussels, Belgium, p 13
- Soerianegara I, Lemmens RHMJ (1993) Timber trees: major commercial timbers. Pudoc, Wageningen, pp 391–434
- Japan Institute of Architecture (2002) Standard for structural design of timber structures, pp 335–337

ORIGINAL ARTICLE

Masahiko Kobayashi · Toshiyuki Asano · Mikio Kajiyama
Bunichiro Tomita

Effect of ozone treatment of wood on its liquefaction

Received: February 4, 2004 / Accepted: June 23, 2004

Abstract The effects of ozone treatment were investigated to improve the process of liquefaction of wood with polyhydric alcohol solvents. The liquefied wood having a high wood to polyhydric alcohol ratio (*W/P* ratio) could be prepared by using the wood treated with ozone in the liquid phase. The liquefied wood with a *W/P* ratio of 2:1 had enough fluidity to act as a raw material for chemical products. To get some information about the effects of ozone treatment toward the wood components, cellulose powder and steamed lignin were treated with ozone and liquefied. In particular, ozone treatment in the liquid phase was found to be effective for wood and cellulose powder. On the other hand, steamed lignin self-condensed during liquefaction after treatment with ozone in the liquid phase. Thus, ozone treatment provided lignin with reactive functional groups, and caused the subsequent condensation reaction. Although lignin was converted to a more condensable structure by ozone treatment, the condensation reaction was found to be suppressed for wood during its liquefaction. The wood liquefied products displayed good solubilities in *N,N*-dimethyl formamide (DMF) even after treatments of long duration. It was suggested that one of the main effects of ozone treatment toward wood was the decomposition of cellulose.

Key words Liquefied wood · Ozone treatment · Cellulose powder · Steamed lignin · Condensation reaction

M. Kobayashi (✉)
Composite Products Laboratory, Department of Wood-Based
Materials, Forestry and Forest Products Research Institute,
1 Matsunosato, Tsukuba 305-8687, Japan
Tel. +81-29-873-3211 (ext. 537); Fax +81-29-874-3270
e-mail: masa7355@fpri.affrc.go.jp

T. Asano
Ibaraki Industrial Technology Center, Ibaraki 311-3116, Japan

M. Kajiyama · B. Tomita
Institute of Agricultural and Forestry Engineering, Faculty of
Agriculture, University of Tsukuba, Tsukuba 305-8572, Japan

Part of this report was presented at the 53rd Annual Meeting of the
Japan Wood Research Society, Fukuoka, April 2003

Introduction

In recent years, much efforts has been expended on the utilization of low-grade woods as a new source of raw materials for preparing resins, and new technologies and products have been developed for the liquefaction of wood.¹ Many studies have pursued the application of liquefied wood to wood adhesives and some molding materials.^{2,3} We have prepared liquefied wood from Japanese cedar, which is expected to be used widely in Japan, and investigated the preparation of liquefied wood/epoxy resin and its application to wood adhesives.^{4,5} One of the most important objects of the application of liquefied wood is increasing the wood contents within final products. However, to date the wood content of liquefied wood is known to be limited to low levels because condensation occurs among the degraded wood components concurrently during liquefaction. It was concluded in our previous report that lignin was solubilized in some organic solvents in the initial stage, followed by liquefaction of cellulose and gradual solubilization, followed by condensation of the liquefied cellulose and lignin to form an insoluble residue.⁶

Ozone is one of the most powerful oxidizing reagents. In this research, ozone was used for the pretreatment of wood before liquefaction so as to activate wood components. It is known that the ozonation of lignin results in derivatives of muconic acid, which have two conjugated double bonds terminated by two carboxyl groups. Because many chemical reactions can be based on these structures, some effects of the liquefaction process can be expected. In particular, because the condensed residue contained a lot of aromatic compounds, it was expected that the condensation might be suppressed by cleaving of the aromatic rings of lignin with ozone. The pretreatment of wood was conducted in the gas phase or in some organic solvents. After that, each ozone-treated wood was liquefied using a mixture of ethylene glycol oligomers and glycerol as solvent. In addition, ozonized cellulose powder and steamed lignin were liquefied, and the processes of their liquefactions were compared with that of wood. The solubilities of the liquefied products in *N,N*-dimethyl formamide (DMF) were examined, and the

molecular weight distributions of their DMF-soluble constituents were evaluated.

Materials and methods

Materials

The heartwood meal of Japanese cedar (*Cryptomeria japonica* D. Don), and the meal of white birch (*Betula platyphylla* Sukatchev var. *japonica* Hara) were prepared, as softwood and hardwood samples, respectively, as raw materials for liquefaction. Cellulose powder (Sigma-Aldrich, USA) and steamed lignin were used as model samples of the main wood components and were also used as raw materials for liquefaction. The steamed lignin was prepared from wood chips of white birch. The chips were steamed for 15 min at 180°C, extracted with water at 60°C, and then extracted with methanol. The methanol-soluble part was dried under vacuum after removal of the methanol, and used as the steamed lignin. All other chemicals were reagent grade, and were used without further purification.

Ozone treatments in gas phase

Each material (15 g) was placed into a 150 liter polyethylene plastic bag after drying at 105°C for 24 h. An ozone generator (DMA-10BDF, Ishimori, Japan) was used with an oxygen flow rate of 500 ml/min, and the generated ozone concentration was 3%. The gas flow was introduced into the bag with shaking for 4.08 h, and the total amount of ozone introduced was 7.7 g. The weight increases after ozone treatments were determined to be 0.065–0.073 g per gram of four kinds of samples: Japanese cedar, white birch, cellulose powder, and steamed lignin. After allowing the samples to stand at room temperature for 1 week, the samples were liquefied in a similar manner as that used for untreated materials.

Ozone treatments in liquid phase

Each material (15 g) was placed into a three-necked 1-liter flask and immersed in a mixture of 1,4-dioxane (300 ml) and methanol (600 ml). The same gas flow as described earlier was bubbled into the solvent with stirring for 4.08 h at 0°C, and the total amount of ozone introduced was 7.7 g. The weight increases after ozone treatments were determined to be 0.229 g, 0.199 g, 0.213 g, and 0.301 g per gram for Japanese cedar, white birch, cellulose powder, and steamed lignin, respectively. After suction drying, the samples were liquefied.

Liquefaction of wood and related compounds

Wood and related samples were dried at 105°C for 24 h before they were used. Each dried sample was placed in a

two-necked flask, equipped with condenser and mechanical stirrer, after it was mixed with polyethylene glycol (average molecular weight 400), glycerol, and sulfuric acid. The weight percentage of glycerol in polyhydric alcohols was 20%. The amount of sulfuric acid used as catalyst was 3 wt% on polyhydric alcohols. The mixing ratios of wood materials and polyhydric alcohol were 2:3. As for the liquefaction of ozone treated Japanese cedar, the mixing ratios were changed to 2:3, 1:1, 3:2, and 2:1. The mixture was reacted at 150°C and small amounts of liquefied product samples were taken at regular intervals during liquefaction. The viscosities of the liquefied products were measured with an Advanced Rheometric Expansion System (Reometric Scientific, USA) at a frequency of 1 Hz.

Measurement of residue content

The extent of liquefaction was evaluated by determining the residual content. Each small sample of liquefied products was diluted with an excess amount of DMF and was filtered off on a GA-100 glass filter paper (Toyo Roshi Kaisha, Japan). Insoluble residues were rinsed with DMF and dried in an oven at 105°C for 24 h. The residue content was determined as the weight percentage of DMF-insoluble residue to the raw starting material.

Fourier transform infrared measurements

Fourier transform infrared (FT-IR) spectra were recorded on a PerkinElmer Paragon 1000 (PerkinElmer, UK) FT-IR spectrometer by using the KBr pellet method.

Gel permeation chromatography analysis

Gel permeation chromatography (GPC) of DMF-soluble components was performed by using a Waters 600E multisolvent delivery system with a Shodex KD-2002 column heated at 50°C, using DMF containing 0.01 M lithium bromide as eluent. Detection was achieved with a differential refractometer (410 Differential Refractometer, Waters, USA). The molecular weights of the liquefied products were roughly estimated based on polyethylene glycol standards.

X-ray diffraction analysis

X-ray diffraction patterns of the samples were recorded on a RINT-Ultima diffractometer (Rigaku, Japan) equipped with a reflection-type goniometer, using CuK α radiation. The crystallinity indexes (CI) were calculated from the ratios of peak areas due to the crystalline region to total area of the X-ray diffraction patterns.⁹

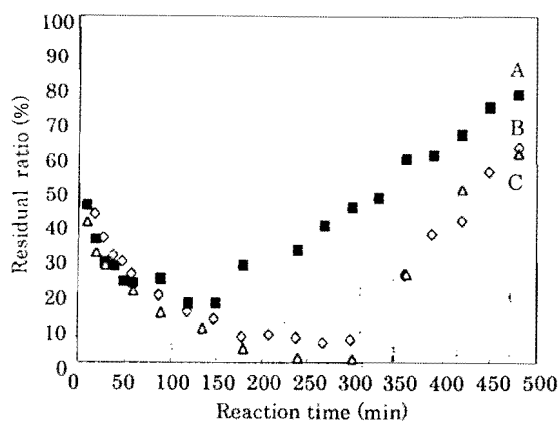


Fig. 1. Dimethyl formamide (DMF) solubility (expressed as residual ratio) of untreated Japanese cedar and ozone-treated Japanese cedar during liquefaction as functions of reaction time, with a wood to polyhydric alcohol ratio (*W/P*) of 2:3. Sample A (squares), untreated Japanese cedar; sample B (diamonds), ozone-treated Japanese cedar in the gas phase; sample C (triangles), ozone-treated Japanese cedar in the liquid phase

Results and discussion

Dissolution behavior of wood and ozone-treated wood

Wood and ozone-treated wood were liquefied, and their dissolution behaviors into DMF were compared. The wood to polyhydric alcohol ratios (*W/P* ratio) were 2:3. In Fig. 1, the curve labeled as sample A (hereinafter expressed as Fig. 1A) shows the dissolution behavior for untreated Japanese cedar as a function of reaction time. The liquefaction proceeded rapidly at the beginning. The residual ratio reached about 20% within 60 min. However, the condensation reaction, which produced insoluble components, took place after 150 min when the minimum residual ratio was observed. It reached 80% at the reaction time of 480 min. Figure 1B shows the results of ozone treatment in the gas phase. The rate of liquefaction was similar to that of untreated wood up to 150 min. However, the residual ratio continued to decrease after 180 min when the condensation reaction started in the case of untreated wood. Subsequently, the residual ratio remained constant at about 5% for the additional 150 min. After 330 min, the condensation progressed abruptly and the residual ratio exceeded 60% at the reaction time of 480 min. Figure 1C shows the results of ozone treatment in the liquid phase. The results were almost the same as those for treatment in the gas phase. However, the minimum residual ratio was further decreased and wood components were completely liquefied within 240 min. It was shown that the condensation could be suppressed to a large extent by ozone treatment. Consequently, the ozone-treated wood was completely liquefied, and its good solubility was maintained for longer than that of the untreated wood. These results suggest that the wood content within the liquefied wood could be increased by using ozone-treated wood. Therefore, preparations of liquefied woods with a higher wood content were attempted

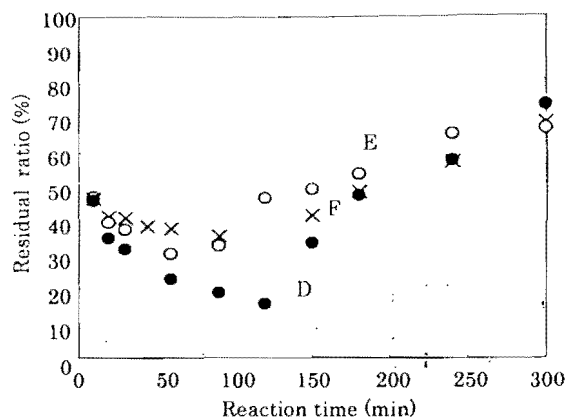


Fig. 2. DMF solubility of ozone-treated wood in the liquid phase during liquefaction as a function of reaction time. Sample D (filled circles), *W/P* ratio 1:1; sample E (circles), *W/P* ratio 3:2; sample F (crosses), *W/P* ratio 2:1

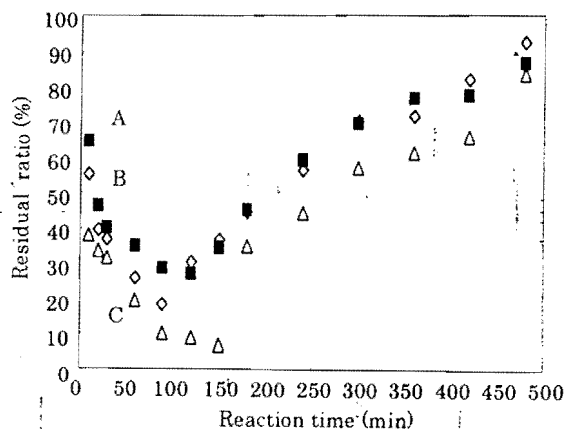


Fig. 3. DMF solubility of untreated white birch and ozone-treated white birch during liquefaction as functions of reaction time, with a *W/P* ratio of 2:3. Sample A (squares), untreated white birch; sample B (diamonds), ozone-treated white birch in the gas phase; sample C (triangles), ozone-treated white birch in the liquid phase

by using ozone treatment in the liquid phase. Figure 2 shows the comparison of the residual ratio during liquefaction with three different *W/P* ratios. In Fig. 2D (*W/P* ratio = 1:1), the residual ratio reached 15% at the liquefaction time of 120 min. Although the liquefied wood contained this amount of residue, it had enough fluidity (1.40×10^3 Pa·s at 25°C) to act as a raw material for chemical products. It should be noted that the liquefied wood with a *W/P* ratio of 1:1 could be prepared by using the ozone treatment without applying other special methods, such as those reported in our previous works.^{4,5} Figure 2E and 2F show the results of the cases with *W/P* ratios of 3:2 and 2:1, respectively. The higher wood content caused the decrease of liquefaction rate. The minimum residual ratios for E and F of Fig. 2 were 30% and 35%, respectively. However, even the liquefied wood which contained more than 66% of wood (*W/P* 2:1) had enough fluidity (5.48×10^3 Pa·s at 25°C) to be used as raw material for chemical products.

Figure 3A shows the liquefaction result for untreated white birch as the function of reaction time. The liquefac-

tion proceeded promptly at the beginning and the residual ratio reached 27% at the reaction time of 120 min. However, the condensation reaction took place at that time, and the residual ratio increased to 90% at 480 min. Figure 3B shows the results of ozone treatment in the gas phase. The liquefaction proceeded faster than in the case of untreated white birch, and the minimum residual ratio was shown at the reaction time of 90 min. After that, the condensation reaction took place and the process proceeded to resemble the case of the untreated sample. Figure 3C shows the results of ozone treatment in the liquid phase. The liquefaction proceeded faster than the untreated and gaseous ozone-treated samples, and the residual ratio reached 6% after 150 min. However, the condensed residue suddenly increased at that point and the residual ratio increased to 35%. Once the residue was formed, the residual ratio increased in a fashion similar to the other two cases. It was shown that the condensation reaction of the liquefied wood for white birch could be suppressed by ozone treatment as in the case of the softwood, and the remarkable effect was observed for the ozonation in the liquid phase.

The ozone-treated hardwood was liquefied faster than the untreated one as mentioned above. However, because the condensation reaction was also enhanced by ozone treatment, complete liquefaction was not achieved. On the other hand, ozone-treated softwood was completely liquefied, and its good solubility was maintained for a wider range of liquefaction periods as shown in Fig. 1. Therefore, it could be said that the ozone treatment was more effective toward the softwood than toward the hardwood.

Influence of ozone treatment on wood raw material

In Fig. 4, A, B, and C show the IR spectra of untreated Japanese cedar, and ozone-treated Japanese cedar in gas and liquid phases, respectively. There was no difference between A and B. This fact suggests that the main functional groups of wood did not change greatly as a

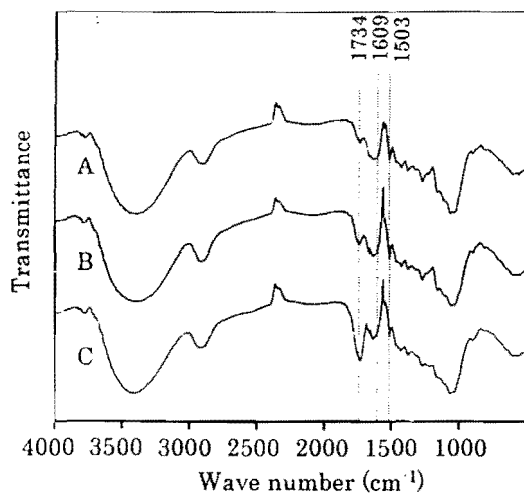


Fig. 4. Infrared (IR) spectra of untreated Japanese cedar and ozone-treated Japanese cedar. Samples A, B, and C as for Fig. 1.

result of ozone treatment in the gas phase. Figure 4C displayed the increase of intensities of the band at around 1730cm^{-1} , showing that carbonyl groups were produced during ozonation. However, further differences were not observed.

In Fig. 5, A, B, and C show the IR spectra of untreated white birch, and ozone-treated samples in gas and liquid phases, respectively. Figure 5B displays a decrease of the intensity of the band at 1609cm^{-1} , showing that the aromatic rings of lignin were cleaved during ozonation. In Fig. 5C, it was observed that the intensity of the band at around 1730cm^{-1} increased in a similar manner as observed for Japanese cedar.

Influence of ozone treatment on molecular weight distribution of liquefied wood during liquefaction

GPC analysis of DMF-soluble material from the liquefaction of untreated Japanese cedar was carried out, and the results are shown in Fig. 6A. Some peaks were observed at the low molecular weight region ($M_w = 400\text{--}1000$) after 10 min of liquefaction. As the reaction proceeded, a peak began to develop in the high molecular weight region ($M_w = 10000\text{--}20000$). After 150 min, when the minimum residual ratio was observed as shown in Fig. 1A, the peaks due to high molecular weight components were clearly detected. Subsequently, as the liquefied products converted to insoluble compounds due to condensation, the peaks became smaller and disappeared by 480 min. Figure 6B shows the results of ozone treatment in the gas phase. It was observed that some peaks were spread over wide ranges toward the lower molecular weight region and more so than in the case of untreated wood. After 90 min, the peak due to high molecular weight components became clearer than in the case of untreated wood. Subsequently, the liquefaction proceeded slowly and the peaks were clearly detected after 300 min when the residual ratio was 5%. Soon afterward, because the condensation reaction took place, the peaks in

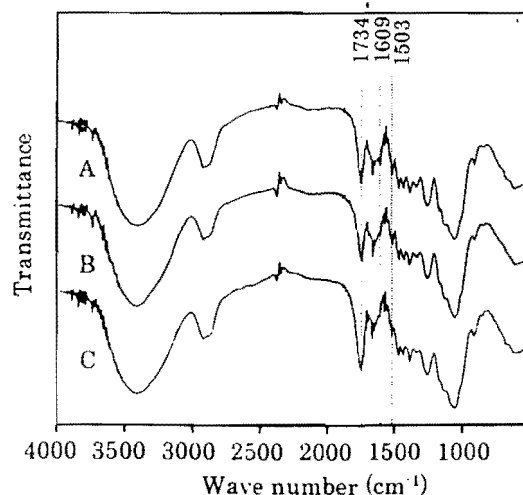


Fig. 5. IR spectra of untreated white birch and ozone-treated white birch. Samples A, B, and C as for Fig. 3.

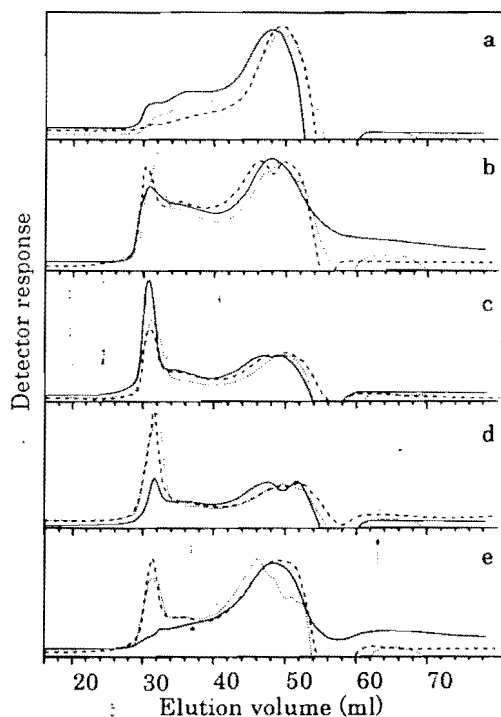


Fig. 6a-e. Gel permeation chromatograms of the DMF-soluble part of liquefied untreated Japanese cedar, ozone-treated Japanese cedar in the gas phase, and ozone-treated Japanese cedar in the liquid phase during liquefaction. Sample A (solid line), untreated Japanese cedar; sample B (long-dashed line), ozone-treated Japanese cedar in the gas phase; sample C (short-dashed line), ozone-treated Japanese cedar in the liquid phase. Liquefaction time: a 10 min, b 90 min, c 150 min, d 300 min, e 480 min.

the high molecular weight region became smaller. However, some of the high molecular weight components remained soluble in DMF. Figure 6C shows the results of ozone treatment in the liquid phase. The change of molecular weight distribution was similar to those found in the treatment in the gas phase.

The results of GPC analysis of untreated white birch are shown in Fig. 7A. The changes of molecular weight distribution were similar to those found for untreated Japanese cedar. Figure 7B shows the results of ozone treatment in the gas phase. After 150 min, although the value of the residual ratio was almost the same as that for untreated sample (Fig. 2), the low molecular weight peaks appeared larger when compared with those of untreated wood. Thus, it can be said that the soluble part of the sample treated with ozone in the gas phase and then liquefied contained larger amounts of low molecular weight constituents than those found for the untreated samples. Figure 7C shows the results of ozone treatment in the liquid phase. After 150 min, when the minimum residual ratio (6.6%) was observed as shown in Fig. 3C, the molecular weight distribution was similar to that of untreated wood (Fig. 7A) in spite of the fact that the residual ratio of untreated wood was 34%. After 300 min, the chromatogram was very similar to that observed for treatment in the gas phase at 150 min (Fig. 7B). These results indicate that the start of the condensation reaction was

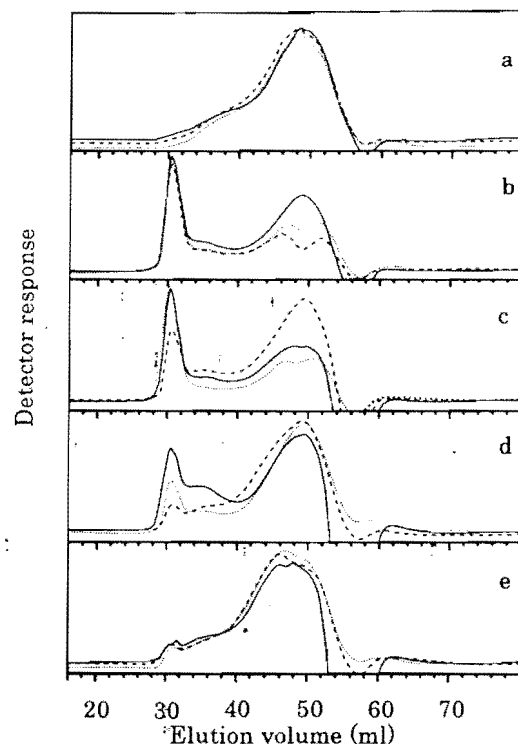


Fig. 7a-e. Gel permeation chromatograms of the DMF-soluble part of liquefied untreated white birch, ozone-treated white birch in the gas phase, and ozone-treated white birch in the liquid phase during liquefaction. Sample A (solid line), untreated white birch; sample B (long-dashed line), ozone-treated white birch in the gas phase; sample C (short-dashed line), ozone-treated white birch in the liquid phase. Liquefaction time: a 10 min, b 90 min, c 150 min, d 300 min, e 480 min.

delayed by ozone treatment in the liquid phase. After that, the peaks in the high molecular weight region ($M_w = 10000-20000$) became smaller and disappeared within 480 min.

Dissolution behavior of untreated and ozone-treated cellulose

Figure 8A shows the DMF solubility of untreated cellulose powder as a function of liquefaction time. Because cellulose powder contains a significant crystalline portion, the rate of liquefaction seemed to be slower than that of wood. After 90 min, 50% of the material remained as insoluble residue. It took 270 min for most of the cellulose powder to dissolve. After that, the residual ratio remained constant at about 10%, and the condensation could not be observed within 480 min. Figure 8B shows the results of ozone treatment in the gas phase. The results are quite similar to those of untreated cellulose. Figure 8C shows the results of ozone treatment in the liquid phase. After 10 min, the residual ratio reached 65%, while it was 90% and 80% for A and B, respectively. The rate of liquefaction was concluded to be faster than A and B, and 80% of the wood components were solubilized within 120 min. Subsequently, the residual ratio decreased as the reaction proceeded, and the residue

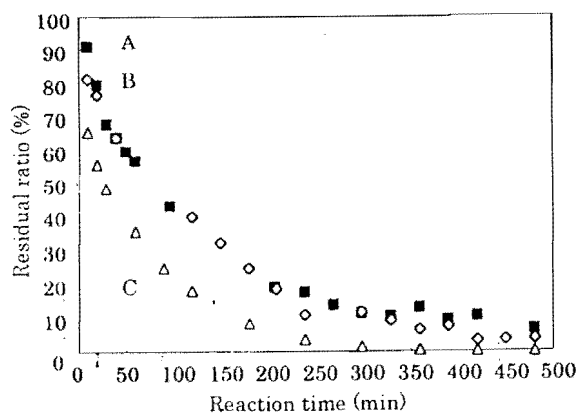


Fig. 8. DMF solubility of untreated cellulose powder and ozone-treated cellulose powder during liquefaction as functions of reaction time. The cellulose powder to polyhydric alcohol ratio was 2:3. Sample A (squares), untreated cellulose powder; sample B (diamonds), ozone-treated cellulose powder in the gas phase; sample C (triangles), ozone-treated cellulose powder in the liquid phase

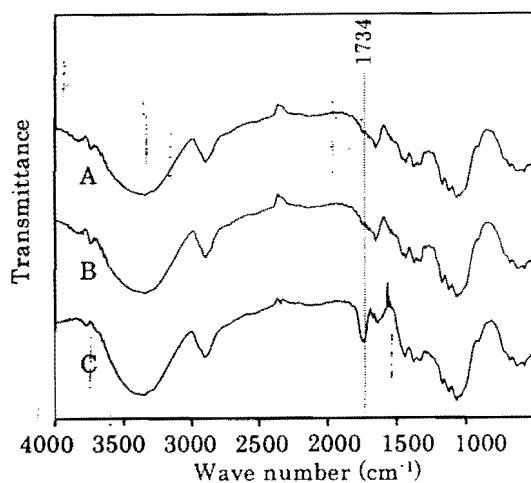


Fig. 9. IR spectra of untreated cellulose powder and ozone-treated cellulose powder. Samples A, B, and C as for Fig. 8

disappeared after 300 min. It was indicated that complete liquefaction was achieved and the ozone treatment effectively acted on cellulose in the liquid phase.

Influence of ozone treatment on cellulose

Figure 9 shows the IR spectra of untreated cellulose (A) and ozone-treated cellulose in the gas (B) and liquid (C) phases, respectively. No difference was observed between A and B. This suggests that the main functional groups of cellulose did not change by the ozone treatment in the gas phase as was recognized in the case of wood. However, the absorption bands appeared at around 1730 cm^{-1} in Fig. 9C. It was reported that when ozone was applied to cellulose, it induced the formation of carbonyl groups and carboxyl groups to a minor extent.¹⁰ Furthermore, it was reported that gluconic acid was the major product in the first stages of

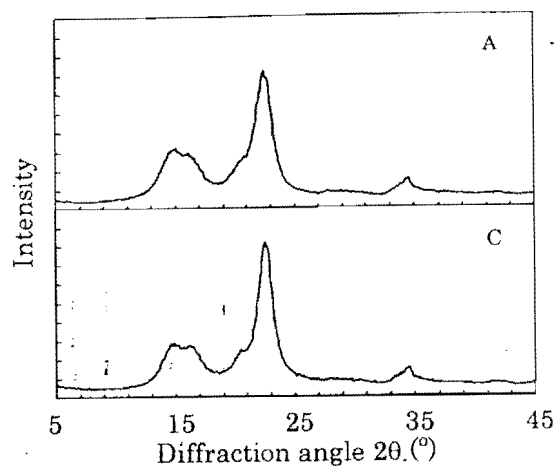


Fig. 10. X-ray diffraction patterns of untreated cellulose powder and ozone-treated cellulose powder. Samples A and C as for Fig. 8

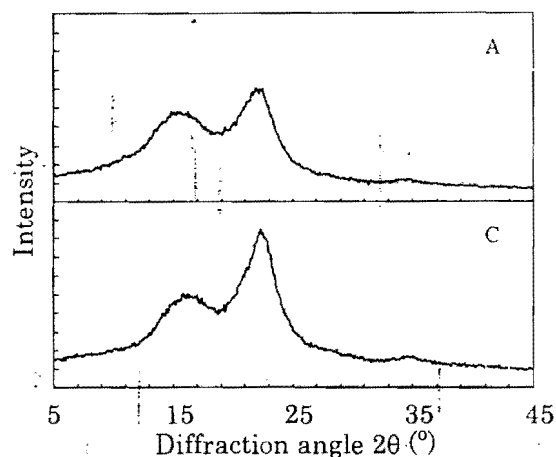


Fig. 11. X-ray diffraction patterns of untreated Japanese cedar and ozone-treated Japanese cedar. Samples A and C as for Fig. 1

ozonation for the model compounds of cellulose.¹¹ This information suggests that the absorption bands at around 1730 cm^{-1} are derived from carboxyl groups which were produced by cleavage of the glycosidic linkage.

To obtain some information about the crystallinity of cellulose, X-ray diffraction of cellulose and wood was carried out. Figure 10 shows the X-ray diffraction patterns of untreated cellulose powder (A) and ozone-treated cellulose powder in the liquid phase (C). It was observed that the peak intensity due to cellulose I increased after ozone treatment.⁹ The CI increased from 35.11% to 37.95%. This suggests that the amorphous cellulose was decomposed by ozone. Figure 11 shows the X-ray diffraction patterns of untreated Japanese cedar (A) and ozone-treated Japanese cedar in the liquid phase (C). The peak area of untreated wood was smaller than that of the ozone-treated material as in the case of cellulose. The CI increased from 17.17% to 18.49% by ozone treatment. Thus, it appears that the amorphous cellulose contained in wood seemed to be influenced

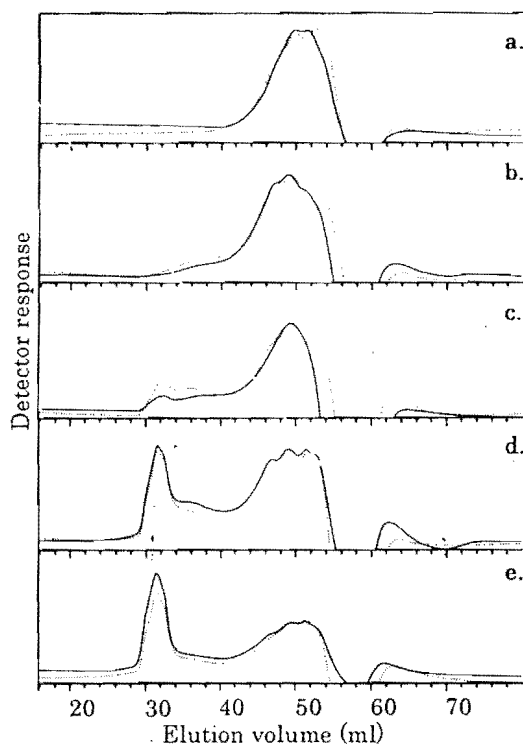


Fig. 12a-e. Gel permeation chromatograms of the DMF-soluble part of liquefied untreated cellulose powder and ozone-treated cellulose powder in the liquid phase during liquefaction. Sample A (solid line), untreated cellulose powder; sample C (short-dashed line), ozone-treated cellulose powder in the liquid phase. Liquefaction time: a 10 min, b 90 min, c 180 min, d 300 min, e 480 min.

by ozone, although it is covered with hemicellulose and lignin, the latter of which is more easily ozonized than cellulose.¹²

Influence of ozone treatment on molecular weight distribution of liquefied cellulose during liquefaction

Figure 12A shows the gel permeation chromatograms of the DMF-soluble part of untreated cellulose powder during liquefaction. In the initial stage of the liquefaction, some peaks were observed in the low molecular weight region ($M_w = 200-1000$). Only the low molecular weight parts of cellulose were liquefied in this stage and converted to DMF-soluble components. The peaks of liquefied products began to develop in the high molecular weight region ($M_w = 10000-20000$) with increased reaction time. The chromatogram obtained after 480 min roughly showed all components of liquefied products, because they were almost all soluble in DMF as shown in Fig. 8A. Figure 12C shows the result of ozone treatment in the liquid phase. The results showed a tendency similar to those of untreated wood from the beginning to the end of the reaction. However, in the initial stages of the liquefaction, the peaks derived from cellulose spread toward the lower molecular weight region ($M_w = 200-400$) than those of untreated cellulose. It was suggested that cellulose was partially decomposed during

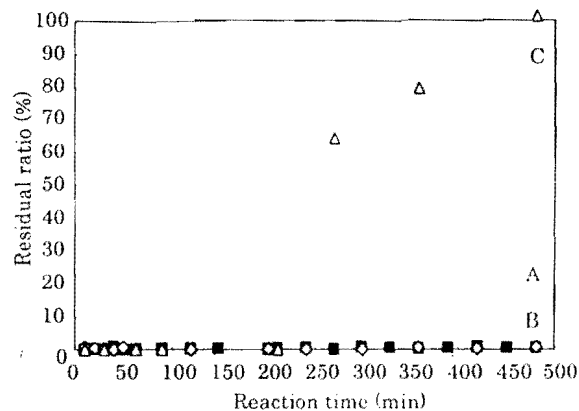


Fig. 13. DMF solubility of untreated steamed lignin and ozone-treated steamed lignin during liquefaction as functions of reaction time. The steamed lignin to polyhydric ratio was 2:3. Sample A (squares), untreated steamed lignin; sample B (diamonds), ozone-treated steamed lignin in the gas phase; sample C (triangles), ozone-treated steamed lignin in the liquid phase.

these processes. Consequently, ozone-treated cellulose was completely liquefied. After 300 min, large peaks were observed in the high molecular weight region as observed in the case of untreated cellulose powder. However, this result indicated that more cellulose could be converted to soluble components by ozone treatment, because the residual ratio was 0% at 300 min, while in the case of untreated cellulose it was 15% at this reaction time. Similarly, the chromatogram showed almost the same pattern as that of untreated cellulose at 480 min, but it was observed that the relative intensity of the peak in the high molecular weight region was a little smaller than that for untreated cellulose.

Dissolution behavior of untreated and ozone-treated lignin

DMF solubilities of untreated steamed lignin and ozone-treated lignin were compared during liquefactions. It was difficult to prepare steamed lignin from softwood such as Japanese cedar. Therefore, white birch was used as raw material. Figure 13A shows the results for untreated steamed lignin as a function of liquefaction time. Untreated steamed lignin is essentially a DMF-soluble compound. Therefore, due to total solubility, the residual ratio was 0% from the beginning of the liquefaction. Although the viscosity of the liquefaction product increased to some extent as the reaction proceeded, the lignin remained completely soluble even after 480 min. Figure 13B shows the results of ozone treatment in the gas phase. Because the lignin was soluble just like untreated lignin, the residual ratio was 0% from the beginning to the end of the liquefaction. Figure 13C shows the results of ozone treatment in the liquid phase and shows an obvious distinction from Fig. 13A or B. The residual ratio was 0% at the beginning, but condensation suddenly took place after 200 min. The residual ratio then increased rapidly and reached 100% at the reaction time of 480 min. Although most wood and cellulose was not soluble

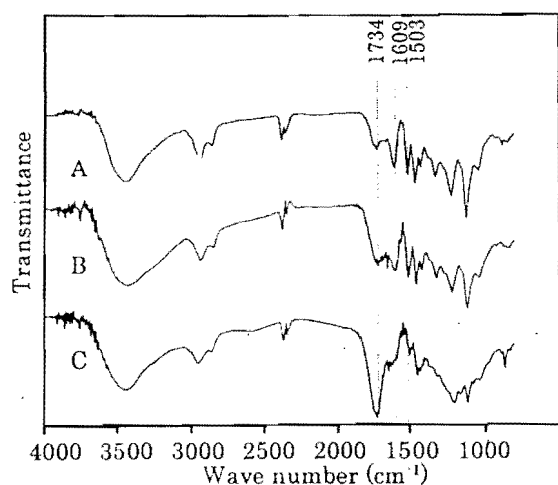


Fig. 14. IR spectra of untreated steamed lignin and ozone-treated steamed lignin. Samples A, B, and C as for Fig. 13

in 1,4-dioxane-methanol after ozone treatment, lignin was completely soluble in this mixture. Consequently, it can be said that ozone reacted with lignin effectively and reactive components were formed.

Influence of ozone treatment on lignin

Figure 14 shows the IR spectra of untreated steamed lignin (A) and ozone-treated lignin in the gas (B) and liquid (C) phases. It was observed that the spectrum pattern of B was similar to that of A. On the other hand, ozone treatment in the liquid phase effected some changes in the main functional groups of lignin, as shown in Fig. 12C. The most visible difference between Fig. 14C and Fig. 14A,B are the presence of strong bands observed at $1720\text{--}1740\text{cm}^{-1}$ derived from $\text{C}=\text{O}$ double bonds. Similarly, the intensities of absorptions at 1503cm^{-1} and 1609cm^{-1} due to the aromatic skeletal vibrations decreased. These facts suggest that the effective ozonation of lignin produced derivatives of muconic acid, which have two conjugated $\text{C}=\text{O}$ double bonds. It could be said that these conversions of lignin structure by ozone treatment trigger the condensation reaction.

Influence of ozone treatment on molecular weight distribution of liquefied lignin during liquefaction

Figure 15A shows the gel permeation chromatograms of the DMF-soluble part of untreated lignin. Because lignin was soluble in DMF as described previously, the chromatogram reflected the behavior of all the components during the liquefaction. The peaks gradually shifted to the high molecular weight region with increasing reaction time. It has been suggested that the lignin self-condenses under acidic conditions.¹¹ Figure 15C shows the results for ozone treatment in the liquid phase. The molecular weight distributions were in the lower molecular weight region when

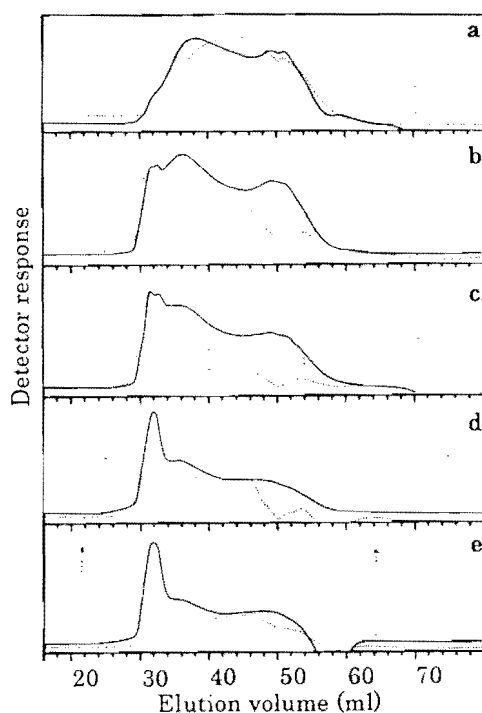


Fig. 15a-e. Gel permeation chromatograms of the DMF-soluble part of liquefied untreated steamed lignin and ozone-treated steamed lignin in the gas phase during liquefaction. Sample A (solid line), untreated steamed lignin; sample C (short-dashed line), ozone-treated steamed lignin in the liquid phase. Liquefaction time: a 10 min, b 90 min, c 180 min, d 300 min, e 480 min

compared with those of untreated lignin at the reaction time of 10 min. However, the distribution shifted much faster to the high molecular weight region than in the case of untreated lignin. After 180 min, the peaks due to high molecular weight components were quite evident. Because the liquefied products were converted to insoluble compounds due to condensation, the high molecular weight peaks became small after 480 min.

Conclusions

In this study, it was found that wood treated with ozone in gas and liquid phases could be liquefied more easily than untreated wood. The liquefied wood with a high W/P ratio of 2:1 could be prepared by using the wood treated with ozone in the liquid phase, and it had enough fluidity to be used as the raw material for chemical products. These results suggest that it was possible to increase the wood contents of final products by using ozone-treated woods. To get some information about the effects of ozone treatment toward the wood components, ozonized cellulose and lignin were also liquefied, and their liquefaction behaviors were observed. Ozone treatment in the liquid phase was effective for wood and cellulose. It was suggested that the amorphous cellulose was decomposed by the treatment. On the other hand, the lignin condensed together during liquefaction when it was ozonized in the liquid phase. This indicated

that the ozone treatment gave lignin reactive functional groups, followed by the condensation reaction. Although lignin converted to a more condensable structure by ozone treatment, the condensation reaction could be suppressed during liquefaction. It was suggested that one of the main effects of ozone treatment toward wood was the decomposition of cellulose.

References

1. Shiraishi N (1986) Plasticization of wood (in Japanese). *Mokuzai Gakkaishi* 32:755-762
2. Lin L, Yoshioka M, Yao Y, Shiraishi N (1995) Preparation and properties of phenolated wood/phenol/formaldehyde cocondensed resin. *J Appl Polym Sci* 58:1297-1304
3. Yao Y, Yoshioka M, Shiraishi N (1995) Rigid polyurethane foams from combined liquefaction mixtures of wood and starch (in Japanese). *Mokuzai Gakkaishi* 41:659-668
4. Kobayashi M, Tsukamoto K, Tomita B (2000) Application of liquefied wood to a new resin system - synthesis and properties of liquefied wood/epoxy resin. *Holzforschung* 54:93-97
5. Kobayashi M, Hatano Y, Tomita B (2001) Viscoelastic properties of liquefied wood/epoxy resin and its bond strength. *Holzforschung* 55:667-671
6. Kobayashi M, Asano T, Kajiyama M, Tomita B (2004) Analysis on process of wood liquefaction with polyhydric alcohol. *J Wood Sci* 50:407-414
7. Kaneko H, Hosoya S, Nakano J (1980) Degradation of lignin with ozone (in Japanese). *Mokuzai Gakkaishi* 26:752-758
8. Yoshida Y, Kajiyama M, Tomita B, Hosoya S (1990) Synthesis of ozonized lignin/aminomaleimide resins using the Diels-Alder reaction and their viscoelastic properties (in Japanese). *Mokuzai Gakkaishi* 36:440-447
9. Isogai A, Usada M (1990) Crystallinity index of cellulosic materials (in Japanese). *Sen-i Gakkaishi* 46:324-329
10. Chirat C, Lachenal D (1994) Effect of ozone on pulp components application to bleaching of kraft pulps. *Holzforschung* 48 Suppl.:133-139
11. Olkkonen C, Tylli H, Forsskahl I, Fuhrmann A, Hausalo T, Tamminen T, Hortling B, Janson J (2000) Degradation of model compounds for cellulose and lignocellulosic pulp during ozonation in aqueous solution. *Holzforschung* 54:397-406
12. Ek M, Gierer J, Jansbo K (1989) Study on the selectivity of bleaching with oxygen-containing species. *Holzforschung* 43:391-396
13. Yasuda S, Terashima N, Ito T (1980) Chemical structures of sulfuric acid lignin I. Chemical structures of condensation products from monolignols (in Japanese). *Mokuzai Gakkaishi* 26:552-557